LETTER

Longitudinal (^{18}F)AV-1451 PET imaging in a patient with frontotemporal dementia due to a Q351R MAPT mutation

INTRODUCTION

Mutations in the microtubule associated protein tau (*MAPT*) gene are a common cause of inherited frontotemporal dementia (FTD) and result in the deposition of pathological tau protein in the brain.[1] Tau positron emission tomography (PET) may enhance in vivo diagnosis and testing of tau-based therapies in FTD, however, few tau ligands have been validated in FTD. The (^{18}F)AV-1451 ligand was developed to assess in vivo tau accumulation and has consistently been shown to bind to tau in individuals with Alzheimer's disease (AD) but less work has focused on the non-AD tauopathies, including FTD. Autoradiography studies of (^{18}F)AV-1451 have shown strong binding in regions of neurofibrillary tangles matching the pattern of paired helical filament (PHF) immunochemistry but have not shown strong binding to non-PHF-tau.[2]

In (^{18}F)AV-1451 studies conducted in FTD spectrum disorders, not only does the ligand not bind strongly to non-PHF tau, but there is significant in vivo binding reported in conditions where no tau is expected at all, for example, in patients with semantic variant primary progressive aphasia and with *C9orf72* expansions where TDP-43 pathology is usually found.[3 4] (^{18}F)AV-1451 also displays both off-target binding in the basal ganglia and an age-related increase in binding in cognitively healthy controls.[3] Nevertheless, this ligand has shown strong binding in a subset of FTD-causing *MAPT* mutations, including V337M and R406W that are associated with PHF-tau pathology.[1 5] (^{18}F)AV-1451 may therefore be useful in detecting tau pathology in some genetic forms of FTD that result in similar structural conformations of tau to that of AD. Here we describe longitudinal (^{18}F)AV-1451 PET imaging from a patient with FTD due to a Q351R mutation located on exon 12 of the *MAPT* gene.[6]

METHODS

Participants

A patient with a Q351R *MAPT* mutation in her mid-60s as well as six healthy controls (three male and three female: mean age at scan 44.7 years, range 29.1–68.3 years) underwent (^{18}F)AV-1451 PET and T1-weighted MR imaging. The Q351R *MAPT* mutation carrier was also scanned 1 year later. All participants gave their consent to take part.

Scanning procedures

All participants were scanned on a Siemens Biograph 6 PET-CT scanner with Truepoint gantry. Dynamic PET data were acquired continuously following intravenous bolus

A

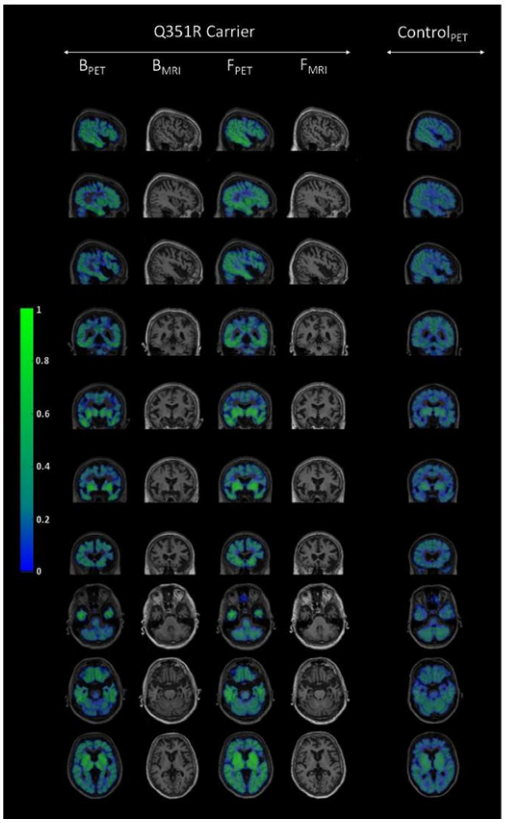

B

BRAIN REGION	CONTROL MAX BP_{ND}	CONTROL MEAN BP_{ND}	CONTROL SD BP_{ND}	Q351R BASELINE BP_{ND}	T-SCORE BASELINE	P-VALUE	Q351R FOLLOW-UP BP_{ND}	T-SCORE FOLLOW-UP	P-VALUE	% INCREASE
CORTICAL										
FRONTAL	0.17	0.07	0.07	0.20	1.68	0.153	0.23	2.17	0.083	19
TEMPORAL	0.23	0.11	0.08	0.32	2.46	0.057	0.41	**3.56***	**0.016**	29
PARIETAL	0.21	0.09	0.09	0.13	0.37	0.728	0.21	1.18	0.293	65
OCCIPITAL	0.23	0.14	0.08	0.15	0.11	0.917	0.33	2.40	0.062	130
CINGULATE	0.25	0.13	0.09	0.23	1.04	0.345	0.26	1.35	0.236	13
INSULA	0.21	0.10	0.06	0.29	**2.82***	**0.037**	0.37	**4.10***	**0.009**	29
SUBCORTICAL										
CAUDATE	0.25	0.05	0.13	0.34	2.03	0.099	0.65	**4.14***	**0.009**	89
PUTAMEN	0.50	0.28	0.15	0.92	**3.97***	**0.011**	1.10	**5.10***	**0.004**	20
PALLIDUM	0.60	0.31	0.19	1.14	**4.11***	**0.009**	1.15	**4.18***	**0.004**	1
MEDIAL TEMPORAL	0.20	0.10	0.08	0.55	**5.48***	**0.003**	0.59	**6.00***	**0.002**	8
THALAMUS	0.40	0.25	0.12	0.47	1.65	0.160	0.61	**2.75***	**0.040**	30

Figure 1 (A) BP_{ND} of (^{18}F)AV-1451 in a Q351R MAPT mutation carrier, at baseline and follow-up 1 year later and a representative age-matched control participant. Sagittal, coronal and axial views are displayed for PET images for all participants, as well as T1-weighted MR images for the mutation carrier. Areas of maximal BP_{ND} in the patient at baseline were the medial temporal, pallidum, putamen and insula regions, with the addition of the temporal cortex, thalamus and caudate at follow-up. (B) BP_{ND} max, mean and SD in controls, with BP_{ND} and T-scores in the patient with the Q351R MAPT mutation at baseline and follow-up, with percentage increase in BP_{ND} between baseline and follow-up. Bold represents a significant difference between the patient and controls. B, baseline; BP_{ND}, non-displaceable binding potential; F, follow-up; max, maximum; MAPT, microtubule associated protein tau; PET, positron emission tomography.

injection of (^{18}F)AV-1451 for 120 mins in 3D-mode. A low-dose CT scan of the head was also acquired.

Dynamic images were reconstructed using a filtered back projection algorithm (direct inversion Fourier transform), with isotropic voxel size of 2 mm^3. Corrections for decay and random counts were performed, and attenuation and scatter were corrected based on the CT scan acquired preceding PET acquisition. Rigid head motion correction using image registration was performed to align the reconstructed dynamic PET frames. Frames affected by mismatched attenuation correction were identified by visual inspection and excluded from kinetic analysis. All participants also underwent T1-weighted volumetric MR imaging on a 3T Siemens Trio scanner.

A simplified reference tissue model (SRTM) with basic functions was used to generate non-displaceable binding potential (BP_{ND}) values. BP_{ND} values were calculated using the pons as a reference region. Regions of interest were defined on the co-registered T1-weighted MR image using a previously described parcellation methodology generating six cortical and five subcortical regions including a combined medial temporal (amygdala and hippocampus) region.[7]

Analyses

T-scores were calculated and differences in BP_{ND} between the carrier (at both baseline and follow-up) and controls were compared using standard single case methodology, with a significance level set at 0.05.

RESULTS

Clinical history

A detailed case report of the patient until the age of 62 has been previously reported.[6] In her mid-60s when she had the baseline PET scan, she carried a diagnosis of behavioural variant FTD. Her disease had been very slowly progressive, initially starting in her mid-40s with an amnestic presentation and quite subtle behavioural change. A change in personality only became prominent in her late 50s. By the mid-60s she was apathetic, but disinhibited at times, with a sweet tooth, and impaired executive function as well as both episodic and semantic memory difficulties. At the time of the baseline scan, her mini-mental state examination (MMSE) was 24/30 and frontotemporal lobar degeneration-modified clinical dementia rating (FTLD-CDR) sum of boxes was 18, while at the follow-up scan, her MMSE had decreased to 18 and her FTLD-CDR had increased to 19.5. Her father developed a similar illness in his 40s, dying at the age of 55. Genetic screening had revealed a novel Q351R mutation (NM_001123066.3: c.2057A>G), not previously reported in other families.

PET imaging analysis

At baseline, the patient's BP_{ND} was higher than the mean control BP_{ND} in all regions, and higher than the maximum control BP_{ND} in the frontal, temporal and insula cortical and all subcortical regions. A significant difference from controls was seen in the insula region cortically, and the medial temporal, putamen and pallidum regions subcortically (figure 1).

At follow-up, the patient's BP_{ND} values had increased across all cortical and subcortical regions after 1 year. These were now higher than the maximum control BP_{ND} in all cortical and subcortical regions, with a significant difference from the control group in the same regions as at baseline but also now the temporal region cortically and caudate and thalamus regions subcortically.

The patient's regional BP_{ND} values negatively correlated with brain volumes both at baseline ($r^2=-0.745$, $p=0.008$) and follow-up ($r^2=-0.791$, $p=0.004$) (Supplementary Table 1, Supplementary Figure 1).

DISCUSSION

In this study, we show increased binding of the (^{18}F)AV-1451 ligand in an individual with a Q351R *MAPT* mutation in both cortical and subcortical regions, with higher binding potential in all regions at longitudinal follow-up later. The findings are consistent with the known pattern of symmetrical anteromedial temporal and insula lobe and basal ganglia involvement seen in *MAPT* carriers.[7]

As with prior studies, we found some binding of the (^{18}F)AV-1451 ligand in healthy controls, particularly centred around the basal ganglia, although this was lower than in the patient, even at the baseline scan. The nature of such off-target binding remains unclear, although it is not likely to represent binding to tau.

There has been little investigation of longitudinal change in (^{18}F)AV-1451 binding. Here we provide evidence that a very variable change is seen over a 1-year interval in a patient with a slowly progressive form of FTD. In cortical regions, the percentage increase varied from 13% to 130%, while in the subcortical regions it varied from 1% to 89%, with the lowest increase seen in the pallidum where the most off-target binding was seen in controls.

No one with a Q351R mutation has yet to come to postmortem. However, the mutation sits between two mutations known to have PHF-tau pathology (V337M and R406W).[2] Strong binding of (^{18}F)AV-1451 has been shown in both mutations in vivo,[5] suggesting that the strong binding observed in this patient is also indicative of PHF-tau pathology, although further studies will be needed.

This study suggests that the (^{18}F)AV-1451 ligand may be a useful biomarker in at least a subset of *MAPT* mutations that result in PHF-tau pathology in FTD. However, further work needs to be done in characterising tau ligands that may be useful across the spread of non-AD tauopathies.

Rhian S Convery,[1] **Jieqing Jiao,**[2] **Mica T M Clarke,**[1] **Katrina M Moore,**[1] **Carolin A M Koriath,**[1] **Ione O C Woollacott,**[1] **Philip S J Weston,**[1] **Roger Gunn,**[3] **Ilan Rabiner,**[3] **David M Cash,**[1] **Martin N Rossor,**[1] **Jason D Warren,**[1] **Nick C Fox,**[1,4] **Sebastien Ourselin,**[2] **Martina Bocchetta,**[1] **Jonathan D Rohrer**[1]

[1]Dementia Research Centre, Department of Neurodegenerative Disease, UCL Institute of Neurology, Queen Square, London, UK
[2]School of Biomedical Engineering and Imaging Sciences, King's College London, London, , UK
[3]Imanova Centre for Imaging Sciences, London, UK
[4]Dementia Research Institute at UCL, London, UK

Correspondence to Dr Jonathan D Rohrer, Dementia Research Centre, UCL Institute of Neurology, London WC1N 3BG, UK; j.rohrer@ucl.ac.uk

Acknowledgements The authors thank Avid Radiopharmaceuticals for use of the tracer.

Contributors JDR, RC and JJ designed this study, analysed the data and wrote the manuscript. MC, KM, CK, IOCW, PW, RG, IR, DC, MR, JDW, NCF, SO and MB helped with data collection, analysis and review of the manuscript.

Funding The Dementia Research Centre is supported by Alzheimer's Research UK, Brain Research Trust and The Wolfson Foundation. This work was supported by the NIHR Queen Square Dementia Biomedical Research Unit and the NIHR UCL/H Biomedical Research Centre, the MRC UK GENFI grant (MR/M023664/1) and the Alzheimer's Society (AS-PG-16-007). This work was conducted using the MRC Dementias Platform UK (MR/L023784/1 and MR/009076/1). JDR is supported by an MRC Clinician Scientist Fellowship (MR/M008525/1) and has received funding from the NIHR Rare Disease Translational Research Collaboration (BRC149/NS/MH). JDW was supported by a Wellcome Trust Senior Clinical Fellowship (091673/Z/10/Z) and his research is supported by the Alzheimer's Society, Alzheimer's Research UK and by the NIHR UCLH Biomedical Research Centre. NCF acknowledges support from the UK Dementia Research Institute at UCL. IOCW was funded by an MRC Clinical Research Training Fellowship (MR/M018288/1). Research Councils UK > Medical Research Council 520874.

Competing interests None declared.

Patient consent for publication Not required.

Ethics approval The study was approved by the local ethics committee.

Provenance and peer review Not commissioned; externally peer reviewed.

► Additional material is published online only. To view please visit the journal online (http://dx.doi.org/10.1136/jnnp-2019-320904).

To cite Convery RS, Jiao J, Clarke MTM, *et al*. *J Neurol Neurosurg Psychiatry* Epub ahead of print: [*please include* Day Month Year]. doi:10.1136/jnnp-2019-320904

Received 8 April 2019
Revised 10 June 2019
Accepted 11 July 2019

J Neurol Neurosurg Psychiatry 2019;**0**:1–3. doi:10.1136/jnnp-2019-320904

REFERENCES

1 Ghetti B, Oblak AL, Boeve BF, *et al*. Invited review: Frontotemporal dementia caused by *microtubule-associated protein tau* gene (*MAPT*) mutations: a chameleon for neuropathology and neuroimaging. *Neuropath Appl Neurobiol* 2015;41:24–46.
2 Marquié M, Normandin MD, Vanderburg CR, *et al*. Validating novel tau positron emission tomography tracer [F-18]-AV-1451 (T807) on postmortem brain tissue. *Ann Neurol* 2015;78:787–800.
3 Bevan-Jones WR, Cope TE, Jones PS, *et al*. [^{18}F]AV-1451 binding in vivo mirrors the expected distribution of TDP-43 pathology in the semantic variant of primary progressive aphasia. *J Neurol Neurosurg Psychiatry* 2018;89:1032–7.
4 Bevan-Jones RW, Cope TE, Jones SP, *et al*. [^{18} F]AV-1451 binding is increased in frontotemporal dementia due to C9orf72 expansion. *Ann Clin Transl Neurol* 2018;5:1292–6.
5 Jones DT, Knopman DS, Graff-Radford J, *et al*. In vivo $_{18}$F-AV-1451 tau PET signal in *MAPT* mutation carriers varies by expected tau isoforms. *Neurology* 2018;90:e947–54.
6 Liang Y, Gordon E, Rohrer J, *et al*. A cognitive chameleon: Lessons from a novel *MAPT* mutation case. *Neurocase* 2014;20:684–94.
7 Rohrer JD, Nicholas JM, Cash DM, *et al*. Presymptomatic cognitive and neuroanatomical changes in genetic frontotemporal dementia in the genetic frontotemporal dementia initiative (GENFI) study: a cross-sectional analysis. *Lancet Neurol* 2015;14:253–62.